CHAPTER VI

TRIGGERING

Report of the Trigger Working Group: *I. Corbett, J. Dorenbosch, E. Eisenhandler, J. Garvey, G. Grayer, J. Hansen, A. Nandi and L. Olsen*

Presented by J. Garvey

REPORT OF THE TRIGGER WORKING GROUP

I. Corbett[a], J. Dorenbosch[b], E. Eisenhandler[c], J. Garvey[d], G. Grayer[a], J. Hansen[e], A. Nandi[a], and L. Olsen[e]

a. Rutherford Appleton Laboratory
b. NIKHEF, Amsterdam
c. Queen Mary College, London
d. University of Birmingham
e. CERN

1. INTRODUCTION

A full description of the machine parameters and expected performance of the Large Hadron Collider can be found elsewhere in these proceedings. Just prior to the workshop two possible scenarios for machine operation were suggested. Some parameters relating to these two possibilities are presented in Table 1. During discussions at the workshop and in this report we will refer to these two possible modes of operation. However it should be clear that postulating specific operating conditions only provides a focus for discussion and in general does not rule out other solutions. Where it is felt that there may be absolute limits to any parameter from the point of view of triggering, then these will be explicitly discussed. In particular in Section 2 we discuss the implications on the trigger of the time between collisions and in Section 3 the consequences of more than one collision per crossing.

Table 1

Some parameters describing the two possible scenarios for the LHC presented by G Brianti at this Workshop

Number of bunches	540	3564
Number of crossing points	8	8
Beta value at crossing point	1	1 m
Beam beam tune shift	0.0025	0.0011
Number of particles/bunch	$7.7*10^{10}$	$1.2*10^{10}$
Normalised emittance	15π	$5\ \pi$ µm
Full bunch length	0.3	0.3 m
Crossing angle	0	48 µrad
Operating energy	8.993	8.993 TeV
Rms beam radius	19.8	11.4 µm
Beam beam lifetime	19.8	43.6 h
Luminosity	$7.3*10^{32}$ cm^{-2} s^{-1}	$3.3*10^{32}$ cm^{-2} s^{-1}
Time between crossings	165	25 ns

Table 2 Possible Theoretical Signatures

Topic	Channel	Production Cross Section at $\sqrt{s}$. 20 TeV	Signature	Trigger Thresholds
Higgs				
Mass 100-200 GeV/c^2	$gg \to H + t\bar{t}$, $q\bar{q} \to H + t\bar{t}$, $H \to t\bar{t}$	350 pb	Many wide jets	~ 100 GeV P_T jet many ~ 50 GeV P_T jets
Mass 200-400 GeV/c^2	$gg \to H \to W^+W^-$, $H \to Z^0Z^0$	$> \frac{1}{10}$ pb	Must be sensitive to Z, W $\to q\bar{q}$ for one boson	~ 100 GeV P_T e^- + 2 jets OR 4 jets
Mass >400 GeV/c^2	WW $\to H \to W^+W^-$, $H \to Z^0Z^0$	$\gtrsim \frac{1}{10}$ pb	ditto But no narrow resonance	ditto
Supersymmetry	$pp \to \tilde{g}\tilde{g} + X$, $\tilde{g} \to q\bar{q}\tilde{\gamma}$	$\gtrsim \frac{1}{10}$ pb	Multi jets + missing E_T	Missing E_T can be > 300 GeV depending on $\tilde{g}$ mass
	$pp \to \tilde{q}\bar{\tilde{q}} + X$, $\tilde{q} \to q + \tilde{g}$, $\tilde{g} \to q\bar{q} + \tilde{\gamma}$ OR $\tilde{q} \to q + \tilde{\gamma}$	$\gtrsim \frac{1}{10}$ pb	Multi jets + missing E_T	Missing E_T can be > 300 GeV depending on $\tilde{g}$ mass
Technicolour	$pp \to P_8^0 + X$, $P_8^0 \to t\bar{t}$	~ 4000 pb	2 wide jets	P_8^0 mass ~ 250 GeV/c^2 ~ 100 GeV P_T jet many ~ 40 GeV P_T jets
	$pp \to V_8^{\pm,0} + X$, $V_8 \to g + (\gamma, Z^0, W^\pm)$	30 pb	jet + neutral energy jet + lepton pair	V_8^0 mass ~ 1000 GeV/c^2 ~ 500 GeV P_T jet + high P_T lepton pair
Compositeness	$gq \to q^*$, $q^* \to qg$	$\gtrsim$ 10 pb	2 jet bump	Masses of excited quarks and leptons unknown
	$q^* \to q + \gamma$	$\gtrsim$ 1 pb	jet + neutral energy bump	
	$q^* \to q + W$	?	3 jet bump, jet + e + ν	
	$q^* \to q + Z^0$	?	3 jet bump, jet + e+e^-	

For a luminosity of 3×10^{32} cm^{-2} s^{-1}, for example, and an inelastic cross-section of 100mb there are 3×10^{7} collisions every second. A small fraction of these collisions contain some interesting physics phenomenon and it is the function of the trigger to recognise these collisions and retain their detailed characteristics for subsequent analysis off line. The trigger selection must be made in a very short time and may have available only rather poor information on the distribution of energy coming from the collision.

For any collision, what are the characteristics which make it interesting and indicate it should be recorded? What is called interesting depends to a certain extent on what theoretical models are in vogue, although elementary constituents produced with high transverse momentum tend to be interesting in a model independent way. The predictions of the currently popular theoretical models are discussed at length in these proceedings. In Table 2 we include a simplified summary, with some details of trigger signatures, which we have extracted from the paper by John Ellis [1].

The present theoretical scenario has several implications for the trigger.

i) The Higgs and technipions may be quite massive. However they decay to bosons and heavy quarks which are themselves unstable. As a result the final event signatures are often complicated and involve many jets, leptons and neutrinos, all of rather modest P_T.

ii) The supersymmetric particles produce large missing E_T with one or two jets of modest P_T (~ 100 GeV/c) and should present few triggering problems.

iii) The composite excited quarks have a simple two jet or jet plus photon decay and present a simple trigger topology.

The variety of interesting physics signatures is large but at the trigger level they all consist of some combination of four categories. This is shown in Table 3.

Table 3

Known final state particles leading to the trigger categories discussed in the text.

Trigger Category	Final State Particle
Jet	Quark or Gluon
Missing E_T	Neutrino or Photino
Localised Electromagnetic Shower	Electron or Photon
Penetrating Particle	Muon

Our philosophy in the trigger working party has been to design a trigger for each of the above four categories separately, each one having its own threshold and multiplicity requirements. Any combination of these triggers can then be required in a versatile way to match the physics signatures corresponding to Table 2 and control the recording of events for further analysis. In this way our physics options are kept completely flexible.

This trigger philosophy and how we envisage it might be implemented are discussed in sections 4, 6 and 7. The conclusions and recommendations of the trigger working party are given in Section 8.

2. PROBLEMS CAUSED BY SHORT TIME BETWEEN COLLISIONS

The LHC is a bunched machine. In this section we consider the consequences to the trigger operation of having bunches very close together and on average one collision per crossing. What is the shortest collision separation time such that the selection of events at the trigger level will not be confused?

The triggers described in Section 1 and more fully in Sections 6 and 7 use calorimetry information as input. These triggers are in fact based on energy distribution around the event vertex for any collision. This means that for each collision the energy deposited in every calorimeter cell or element must be known. There are several approaches possible to achieve this situation.

The simplest and most desirable situation is that the pulses from the calorimeters are sufficiently narrow that they have returned to zero pulse height before the next machine crossing. This is shown diagramatically in Figure 1b. With such pulses the energy in any combination of calorimeter elements can be obtained by a simple analogue adding of the appropriate signals, and the resulting pulse can be required to fulfil certain amplitude requirements, if it is to provide a trigger. This is clearly a "real time" operation which can be pipelined, the only requirement being that each subsequent operation on these pulses be complete in a time less than the time between collisions.

Unfortunately calorimeter pulses which rise and fall in times like 25ns or less are hard to achieve. More typically they may rise in ~ 10ns and fall in ~ 70ns as shown in Figure 1c. The extraction of the energy per calorimeter cell for each collision in this situation depends on a further quantity, the probability of a cell being hit in any collision. Below we investigate the implications of low hit probability and high hit probability.

Suppose the hit probability is low, a few percent. That is to say that in a particular calorimeter cell there is a small probability of pulse overlap. In this case it is still possible to implement the simple "real time" analogue adding of pulses, described above for the idealised situation. However now the pulses must be clipped to a length less than a bunch spacing as indicated in Figure 1d. Depending on the pulse shape the peak amplitude of this clipped pulse will be equal to some fraction of the peak amplitude of the unclipped pulse. If the rise time is less than the clipping time this fraction will be unity. Even if the fraction is much less than unity, if the pulse shape is amplitude independent, the effective energy resolution of the subsequent peak measurement may not be too seriously degraded. If this loss of energy resolution at the trigger level caused by clipping the pulse is unacceptable, a more sophisticated approach is required to extract the summed pulse height produced in any collision from a set of calorimeter elements. We can no longer simply add together the pulses from the chosen set, as at any time this will include the tails of pulses from elements hit in previous collisions and fronts of pulses from elements hit in subsequent collisions. For a given collision, to form the effective energy sum for a set of calorimeter elements, we must

only add together elements which have pulses rising during the period between this collision and the next. Referring again to Figure 1, in forming energy sums of sets of calorimeter elements we must not allow le and lf to enter such a sum as these elements were not struck by particles from the same collision as produced lc. If no clipping is done, then in forming sums of calorimeter elements for triggering purposes, only elements with pulses from a given collision must be included. In the second level trigger described in Section 7 this is the philosophy employed.

Now let us suppose the probability of a calorimeter cell being hit in any collision is high. Then for long pulses the situation at the trigger level is even more difficult. The rise time of the pulses has now certainly to be less than the collision separation time. Pulse shapes like that in Figure lg will be common from a single cell. Obviously a considerable amount of processing must be done on each cell to extract the appropriate pulse height produced in any collision. These pulse heights can then be added to form cell combinations for triggering. This kind of operation will be time consuming and is not really appropriate for the first level of any trigger system. For calorimeter elements with high hit probability the only practical solution to allow triggering is the one where the pulse length is less than the time between collisions.

In Table 4 we show the timing properties of various calorimeter types.

Table 4

Timing properties of various calorimeters

Type	Jitter (small cells)	Rise time	Pulse width
Lead glass	± 2ns	$\leq$ 5ns	~ 40ns
Scintillator sampling with wavelength shifter	± 2ns	~ 10ns	70 - 100ns
Scintillator sampling with fast wavelength shifter	± 2ns	~ 5ns	20ns
Gas sampling (MWPC)	20ns/mm	~ 10ns	$\gtrsim$ 100ns
Liquid Argon	$\leq$ 5ns	50ns	Several 100ns
Liquid Argon + Methane	$\leq$ 5ns	25ns	Several 100ns
Silicon sampling	$\leq$ 5ns	5ns	~ 20ns

3. PROBLEMS CAUSED BY MULTIPLE COLLISIONS PER CROSSING

For a given current of circulating protons more luminosity can be obtained by having fewer bunches. For instance the second scenario for LHC has a luminosity of $\sim 7 \times 10^{32}$ cm^{-2} s^{-1}, these are a bunch spacing of ~ 165ns, and an average of ~ 20 collisions per bunch crossing. Is it possible to do any useful physics with such a machine environment?

This question has been addressed by the jet working party at this workshop and also by the Berkeley Workshop[2]. The conclusion of both investigations is that for simple topologies and in particular single jet events the presence of many minimum bias events does not affect the jet detection. This is particularly true if only calorimeter cells above a certain threshold in transverse energy are allowed to contribute to the "event". This is shown in Figure 2.

It has been argued that it may be possible to disentangle multiple collisions offline by use of tracking chambers. For LHC the vertices will be distributed over a distance of 30 cm FWHM and so in principle it may be possible to see the multiple vertices in the event and separate them out. With precise pointing calorimeters it may even be possible to allocate calorimeter hits to individual vertices but this seems very difficult. If it is possible then the missing transverse energy vector can be constructed for the vertex of interest. This is a very ambitious aim and probably more exotic signatures e.g. jet plus missing E_T, will not be clearly separable from the multiple minimum bias background.

Separation of exotic signatures in a background of many minimum bias events may be possible to a certain extent off-line. However it is certainly impossible at the trigger level where there is no vertex information available and certainly no pointing information from the calorimeters. At the trigger level all the energy detected at one crossing is associated with one collision and quantities like missing E_T and electromagnetic cluster multiplicity, for example, are calculated accordingly. We are convinced that multiple collisions per crossing would lead to confusion and lack of discrimination at the trigger level, for all but simple event topologies.

The preference of the trigger group is to have ≤ 1 collision per crossing on average and specifically the 25ns bunch spacing scenario of Table 1 is the preferred one. For higher luminosities we would go in the direction of smaller bunch spacing and deal with the triggering problem as indicated in Section 2.

4. TRIGGER OVERVIEW

The raw inelastic collision rate at a luminosity of $3 \times 10^{32}\ cm^{-2}\ s^{-1}$, assuming an inelastic cross-section of 100mb, is 3×10^7 per second. To keep the time spent on off line analysis down to a reasonable level only one of these collisions should be recorded. This represents an enormous reduction at the trigger level. For comparison the rejection factor used by UA1 and UA2 running on the CERN Collider has so far reached a value of $\sim 3 \times 10^3$.

To obtain this rejection we propose a three level trigger the details of which are shown in Table 5.

Table 5

Details of the proposed three level trigger

Trigger Level	Decision Time	Input Rate (Hz)	Output Rate (Hz)	Deadtime
1	~ 100ns (pipelined every 25ns)	5×10^7	$< 10^5$	0
2	$\lesssim$ 10 μs	$\lesssim 10^5$	200-1000	~ 0
3	Parallel processing (~ 1s per event)	200-1000	~ 1	~ 0

We show in Section 6 that a first-level trigger matching the 25ns bunch spacing, and hence having no dead-time, is feasible. This trigger uses analogue signals from the calorimeters and digital information from the muon chambers. The second-level trigger described in Section 7 is more sophisticated and precise. It is also based on the calorimeter signals but makes use of these signals in their final digitized form. The time requirement for this trigger limits the rate at which it can accept events from the first-level trigger. We aim to keep this time to less than 10 μs and so the first level output rate must be less than 10^5 per second. The natural choice for a third-level trigger involves not only the calorimeters but combinations of other detector elements, and uses computers, with a resultant timescale of milliseconds. This then is an area where triggering and data acquisition overlap The data acquisition system, described elsewhere in these proceedings, reads out the full event and uses a large number of powerful computers working in parallel to process 200-1000 events per second. This defines for us the output rate of our second-level trigger as indicated in Table 5.

Rather than try to respond to any particular event signature of current theoretical models, we have tried to design triggers for the various end products they have in common, namely jets, electromagnetic showers, missing transverse energy and muons. In addition we can provide a total transverse energy trigger. We then allow as much flexibility as possible in combining them to select events.

The basic algorithms we have considered as entering into these triggers are indicated below. The two trigger processors to be described will have the ability to carry out all these, and form combinations of the results with any other external information available at the end of the processing time.

Hadronic jets

This trigger is based on localised energy depositions in the calorimeters exceeding some energy threshold. Jets are a clear feature of events at the collider, and may be even sharper at the LHC. As a signature for quarks and gluons they are clearly important for triggering.

Electrons and photons

This important trigger is based on highly localised energy deposition in the electromagnetic calorimeter. The detection of electrons in jets, although extremely difficult, should not be excluded at the trigger level.

Missing transverse energy

Actually, the quantity calculated is missing transverse momentum, defined as:

$$\left[\left(\sum_i E_T^i \sin\phi^i\right)^2 + \left(\sum_i E_T^i \cos\phi^i\right)^2\right]^{\frac{1}{2}}$$

where the summation is over all calorimeter cells.

As a signal for non-interacting particles (neutrinos, photinos...) this quantity exceeding some threshold will be an important trigger. Note that muons are also included in this trigger, as their true energy is not deposited in the calorimeters. Missing E_T has a resolution of $0.7\sqrt{\sum_i E_T^i}$ for minimum bias events in UA1. To be sensitive at the LHC, hermeticity of the calorimetry must be retained to small angles with the beam, see Fig. 3, and the calorimeter must have equal electromagnetic and hadronic response.

Total transverse energy

Though extensively used at the $p\bar{p}$ collider to recognise high activity events, this is considered as probably too unselective to be used alone at the LHC. To obtain a reasonable rate, the threshold would have to be set so high that much physics would be lost. It might however be useful in combination with other triggers.

Total energy

This is not a trigger, but by measuring the total energy in the event, multiple interactions (which will be frequent) could be flagged and possibly rejected.

The question of granularity of the electromagnetic and hadronic calorimeters to be used in an experiment at LHC was discussed by the electron-photon and jet working groups at this workshop. We give in Table 6 a possible set of calorimeter cell sizes based on their proposals. For first-level and second-level triggers we attempt to reduce the number of independent cells by adding together their output pulses to form trigger cells.

For jets the trigger cell size is determined by the lateral size of the jet. To contain all the fragmentation particles of a jet, cone half angles of ~ 1 radian are necessary. However 50% of the energy flow is contained in a cone half angle of $\sim 5°$ [3]. For jet triggers we add four hadron calorimeter cells to the appropriate electromagnetic calorimeter cells in front to form cells 10° x 0.2 $(\Delta\phi \times \Delta\eta)$ at first level. For second level we retain the full granularity of the hadron calorimeter cells for the trigger.

For electrons and photons the small lateral size of electromagnetic showers allows very selective triggering against hadron showers. We retain the granularity of the electromagnetic calorimeter cells for the second level trigger. This results in a large number of trigger cells but should lead to the possibility of keeping the electromagnetic trigger threshold down to a low value. For the first level trigger we combine 100 calorimeter cells to form trigger cells of dimensions 5° x 0.1 $(\Delta\phi \times \Delta\eta)$.

Table 6

Calorimeter and trigger cell sizes, $|\eta| < 2.5$

	Electromagnetic Calorimeter -e/γ Trigger	Hadron Calorimeter Jet Trigger
Calorimeter cell size: $\Delta\phi \times \Delta\eta$	$\frac{1}{2}° \times 0.01$	$5° \times 0.1$
No cells per sampling (approx)	360 K	3600
First-level trigger cell size: $\Delta\phi \times \Delta\eta$	$5° \times 0.1$	$10° \times 0.2$
No channels (Analogue)	3600	900
Second-level trigger cell size: $\Delta\phi \times \Delta\eta$	$\frac{1}{2}° \times 0.01$	$5° \times 0.1$
No channels (Digital)	360 K	3600
Third-level trigger	Full detector information	

The jet working group have estimated that for minimum-bias events at a pseudo-rapidity of zero, the hadron calorimeter cell occupancy is less than 0.01 per event. This means that second level trigger cells have a very small probability of pulse overlap even for pulses ~ 100ns long.

5. RATES

Trigger rates are extremely hard to estimate, and in any case we must be wary of building all our expectations on details of a particular model, e.g. jet fragmentation in the ISAJET Monte-Carlo program. We will therefore give only an indication of trigger thresholds which might produce acceptable rates into the data acquisition system and third-level trigger.

Jet triggers

The cross-section is of course very large, see Fig. 4. Our cluster logic at second level picks up most of the energy in a jet. In a 100 GeV bin around a jet transverse energy of 500 GeV the jet rate is about 1/3 Hz at a luminosity of $3 \times 10^{32}\ cm^{-2}s^{-1}$, a c.m. energy of 20 TeV and an acceptance of $\Delta\eta = 1$. A trigger threshold of ~ 200 GeV transverse energy at level two would send about 100 events per second to level three, while a threshold of around 50 GeV would probably be adequate at level one. It is clear that any physics requirement for jet triggers below several hundred GeV transverse energy will be forced to rely on combinations with other signals, e.g. more than one jet, electromagnetic showers, missing transverse energy, etc.

Electromagnetic triggers

The cross-section for jet triggers at $\sqrt{s}$ = 20 TeV is given in Fig. 4. The cross-section for high P_T electrons and photons is expected to be very much smaller. Since an electromagnetic trigger is simply a highly localised energy deposition trigger rates for electrons and photons are completely dominated by jets. When we estimate energy deposition in trigger cells smaller than the size of jets we are dependent on models of sub-jet structure. This means that any calculation of rates as a function of energy can have a very large error.

In the first level trigger we look for energy deposition in the electromagnetic part of the calorimeters, with a cell size which accepts about $\frac{1}{4}$ of the total energy in a jet. We estimate that at a luminosity of 3 x 10^{32} cm^{-2} s^{-1} and an energy of 20 TeV we need to impose an E_T threshold of 16 GeV plus or minus a factor of as much as 2 in order to reduce the rate to 10^4 Hz. The uncertainty is due mainly to details of the jet fragmentation and to the precision of the clipped first-level trigger pulses.

At the second level we do better by using smaller trigger cells, but the limit here is really the number of channels we can handle. As indicated in Table 6 we have suggested retaining the fine modularity of the electromagnetic calorimeter at the second level. ISAJET studies show that these smaller trigger cells probably gain us a factor ~ 5 in rate, and we probably gain another factor, say 1.5, from the better precision of the signals. If we are trying to trigger on electrons in jets this is as far as we can go. Therefore, we can only count on getting an acceptable rate if we use a fairly high threshold, perhaps 50 GeV, E_T. On the other hand, if we are trying to trigger on single electrons or photons we have two other constraints we can use. The first is isolation: in addition to a localized cluster we can demand no activity in the adjacent cells. Experience in UA1 and UA2 indicates that this might gain a factor of 5 or more in the rate. The second is the shape of the shower profile in depth: we can demand an electromagnetic shower profile. Detailed shape fitting is best left for the third-level trigger, but at second level we can easily require that there be no signal in the hadron calorimeter behind the struck e.m. calorimeter cell. This should gain us a factor of around 10 (again based on UA1 and UA2 experience), so that we have a total factor of at least 10^2 at second level in triggering on isolated e.m. showers. This keeps our nominal E_T threshold of 16 GeV acceptable through to the third-level trigger.

Missing transverse energy triggers

It is even harder to estimate rates for a missing transverse energy trigger. In UA1 the resolution on missing E_T is given by 0.7 $\sqrt{\Sigma E_T}$, and is limited by gaps in the calorimeter and the different e.m. and hadronic response of the calorimetry. This can be improved by better design and by the use of fission-compensated (for example, uranium) calorimeters. Hermeticity of the calorimetry down to small angles is also an important consideration for missing E_T resolution. In fig. 3 we show the result if an ISAJET calculation showing how missing E_T depends on the minimum angle which is provided with calorimetry.

6. FIRST-LEVEL TRIGGER

The first-level trigger uses analogue signals from the calorimeters. We keep zero dead-time in the first level trigger by using pipelining techniques. As already indicated in section 2 the calorimeter pulses are clipped to less than 25ns. Once this is done the propagation delay of the trigger logic can be > 25ns (we estimate 100ns) as long as the signals can be fed in and ripple through every 25ns. A block diagram is shown in Figure 5. The pulse from each of the calorimeter cells is clocked through a flash ADC and into a shift register at ~ 200 MHz. If after ~ 100 ns the first level trigger says that the event is to be kept then the flash ADC values are clocked into a buffer memory. If not they fall off the end of the switch register. These digitized pulse heights are the ones to be recorded for off-line analysis. They are also to be used by the second-level trigger.

The first-level trigger is meant to reduce the overall trigger rate from the order of 3×10^7/sec to roughly 10^5/sec in 100 ns. For this purpose it is not necessary to have very fine granularity or a perfect energy resolution. We define an e/γ trigger cell as the analogue sum of 10 x 10 primary electromagnetic cells (table 5), summed over the three samplings in depth. The total number of trigger cells to consider, in the first-level trigger, is reduced to 3600 $5° \times 0.1(\Delta\phi \times \Delta\eta)$ cells.

Similarly the signals from four hadronic calorimeter cells and the corresponding four electromagnetic trigger cells are analogue added to form a $10° \times 0.2(\Delta\phi \times \Delta\eta)$ hadronic trigger cell. The electromagnetic and hadronic compartments are added with the appropriate weights if necessary. The total number of hadronic trigger cells is of the order of 900.

All the resulting analogue signals are split into three streams with weights proportional to $\sin(\theta)$, $\sin(\theta)\cos(\phi)$ and $\sin(\theta)\sin(\phi)$, (E_T, E_x and E_y).

A set of subtriggers is then defined, which later on can be combined in any desirable way:

i) electron or photon
Any electromagnetic trigger cell with transverse energy in excess of some computer adjustable threshold.

ii) jet
Any hadronic trigger cell with transverse energy in excess of some computer adjustable threshold.

iii) $\Sigma|E_T|$
The analogue sum of transverse hadronic energy exceeding some computer adjustable threshold.

iv) Missing E_T
$(\Sigma E_x + \Sigma E_y)$ greater than some computer adjustable threshold. Notice that at first level ΣE_x and ΣE_y are merely added.

As well as these calorimeter triggers we must have the muon trigger at the first level. This is described in the contribution of the muon working group in these proceedings.

7. SECOND-LEVEL TRIGGER

The second level trigger has available approximately 10μs per event. The information available and assimilable in this time consists of fully digitized calorimeter pulse heights and muon track information. Track information from a central tracking chamber may be available but we feel its use is more appropriate to the level three trigger (see contribution of Data Acquisition working group). Nor is it considered possible to utilise transition radiation detector signals at this level. The muon trigger is discussed elsewhere in these proceedings.

The trigger we will describe uses the calorimeter signals only. However this trigger differs from the level one trigger in that it uses smaller trigger cells and fully digitized signals (Table 6).

7.1 Digitization

The details of the digitization of the calorimeter cell pulse heights will be described here. The digitization is to be achieved using FADC's and digital accumulators and is shown schematically in Fig. 6. The analogue signal from each detector cell is digitized every 5ns and clocked through a shift register 125ns long. After 100ns from the time of the machine crossing the decision from the first-level trigger is available and if the event is to be kept for second-level processing the FADC digitizings are clocked into a buffer memory. After a further time of 125ns this memory contains the pulse height information for this cell covering the period -25ns to + 100ns relative to the time of the machine crossing which produced the first-level trigger. If the collision is not to be kept then the FADC digitizings fall off the end of the shift register and are discarded. The memory can hold digitized pulse heights for up to say five events. This memory represents a de-randomising event buffer which guarantees zero dead-time for the second-level trigger.

When the second-level trigger processor is available to process the next event retained in memory, the FADC values are clocked into a fast accumulator where the integrated pulse area is obtained in digital form. The memory locations are not cleared in this operation as they may be required to be transferred to the third-level trigger if the event is accepted by the second level.

It is at this point in the operation of the trigger, i.e. as the 5n.s. spaced FADC digitizings are being clocked into the accumulator, that detection of early or late pulses in any cell can be made (see Fig. 1e,f). We have considered two possible ways of reducing the effect of such pulses if they exist. The first solution is to sample the pulse in the periods -25ns to 0ns and 25ns to 50ns and apply a simple correction. The -25ns to 0ns measurement is akin to a "pedestal" subtraction. The second solution is more drastic but probably simpler to apply. If the integrated pulse height in the period -25ns to 0ns is greater than some threshold, or in the period 0ns to 25.0ns less than same threshold then the cell in question is not sent to the second-level adding tree. This solution is probably acceptable where cell occupancy per event is low.

7.2 Cluster algorithms

In Section 4 we discussed the granularity of trigger cells for the second-level

trigger. Here we wish to indicate how we intend combining these trigger cells to achieve the best trigger selectivity.

For the electron-photon trigger there are three characteristics which improve rejection of hadrons. These are the high localisation, isolation and low penetration of electromagnetic showers. Two of these, isolation and low penetration, are of course not usable if it is required to trigger on electrons in jets. We have decided to go for the best trigger cell granularity to benefit most from localisation but have retained the possibility in the trigger of requiring low penetration and isolation.

To allow for showers overlapping calorimeter cell boundaries, combinations of four calorimeter cells must be taken to form one electromagnetic trigger cell. This results in just as many cells however, each of which must be provided with an energy comparator. To reduce the electronics required, channels could perhaps be multiplexed, so that one comparator serially services say ten electromagnetic channels. This multiplexing could take place in parallel with the other trigger functions of the processor.

The way we envisage finding jets is to look for contiguous clusters of calorimeter cells in which some (low) energy threshold is exceeded. This should result in account being taken of different dimension jets, and lead to a more accurate separation and multiplicity evaluation of jets. One possible way of doing this is using the approach of CDF[4]. Obviously the cell size must be large enough, and the threshold low enough, to avoid splitting jets. Another adjustable parameter is the definition of contiguity of cells; either a weak definition (only cells having a common "side" in (psuedo-rapidity, phi) space are contiguous, i.e. each cell has four contiguous neighbours), or a strong definition (in which all eight neighbouring cells are considered as contiguous) may be taken. Optimisation of these parameters was considered as being outside the scope of this Workshop. An extensive Monte-Carlo study of the range of possibilities would clearly be required.

7.3 Processor operation

The basis of the processor is a summing tree which adds the contributions from every trigger channel in the experiment, and stores the value for later evaluation. These channels would however be gated from a number of different sources, so that only the sum appropriate to the desired trigger appears at the output. The incoming calorimeter pulse height digitisation would be converted to processor units representing energy E, transverse energy E_T, and the projections $E_T \sin\phi$ and $E_T \cos\phi$ by selecting one of four memory banks (RAM) look-up tables according to the quantity required by the algorithm being evaluated at the time (see Figure 7). The whole would be controlled by a micro-program (controlling registers) which cycle through the sequence of triggers required, storing the results of each in registers. At the end of the sequence, fast final logic would make choices on the basis of information held in the registers, and possibly other external information, to make a final accept or reject decision.

To clarify the operation of the processor, each trigger implementation will be described in turn.

Total energy

The memory banks are set to E. All trigger channel gates are set on by the program

registers. The total energy in the crossing gate is evaluated, and a comparator may be set to reject the data at this stage if it is considered that too many interactions took place during the crossing for analysis.

Missing transverse energy

The memory banks are switched to $E_T \sin\phi$ and subsequently $E_T \cos\phi$, with all channels still gated on (or possibly some of the calorimetry at small angles to the beam excluded). These sums are recorded in registers, and then fast multiply/summing circuits evaluate the sum of the squares.

Total transverse energy

The memory banks for E_T are selected, with all the gates on, and the transverse energy sum evaluated and stored.

Jet trigger

With E_T selected, the output of a comparator set at a low threshold records in registers cells exceeding this threshold. Cluster logic then sequentially searches for jets. Each cluster is used to gate the adding tree, then the memory banks switched, so that the E, E_T, $E_T \sin\phi$ and $E_T \cos\phi$ for each jet may be recorded. From this the mean values of θ and ϕ for the jet may be deduced. As each jet is found, the cells are removed by re-setting the register bits corresponding to the contributing cells.

Electron trigger

As can be seen from Figure 7, each electromagnetic trigger cell has two comparators. These comparators are connected to registers in which the patterns of hits are stored. The multiplicity of hits for two comparator thresholds can obviously be obtained using simple logic. If an isolation requirement is invoked then this can be achieved by a suitable choice of comparator thresholds and a logical analysis of the two hit patterns. Of course the hit patterns for the electromagnetic trigger cells contain 360 K bits. The multiplicity and isolation logic might be split into 3600 100-bit patterns without any loss of generality. These groups of 100 electromagnetic cells will be chosen to be matched to the hadron calorimeter trigger behind. A comparator on each hadron cell can then be used to veto any electromagnetic deposition and provide if necessary a low penetration requirement on the electron trigger.

7.5 Processor timing

In view of the large number of serial operations mentioned above, the question of timing is naturally raised. The propagation through the summing tree could be quite short, less than 100ns, but the relevant number is rather the settling time of the circuitry, since in principle the operations could be pipelined. More parallelism than has been outlined here may be necessary, for example the four memory banks could each have their own summing tree and could operate in parallel. Electron candidate searching (multiplexing) could go on in parallel with other operations, as possibly could jet searching. Jet cluster logic of the type described here is at present being built for the CDF detector at Fermilab, and a time of about 230ns per cluster is estimated for their experiment.

8. CONCLUSIONS

1) We strongly favour machine designs with an average of ≤ 1 collision per bunch crossing. Triggering on complicated signatures (necessary for the predicted physics) does not seem feasible in a multi-event environment.

2) The short bunch spacings ($\sim$ 25ns) required to achieve ≤ 1 collision per crossing at high luminosity make it necessary that the calorimeters have fast-rising pulses of short overall length. The calorimeter cell sizes should be small enough to restrict average cell occupancy per crossing to a few per cent at most.

3) Electron-photon triggers can be made very selective in the case of isolated showers. To trigger on electrons or photons inside jets is much more difficult and will require the use of higher energy thresholds. Very large numbers of trigger channels must be handled in order to take advantage of the small lateral size of electromagnetic showers.

4) The trigger system we have described is very expensive at 1984 prices. However, we feel that in the next ten years development of fast integrated circuits will bring this down to a more modest level.

5) Highly selective triggering appears to be feasible, but must take full advantage of the predicted event topologies to keep energy thresholds as low as possible. One must therefore look for combinations of jets, electromagnetic showers, muons and missing energy.

* * *

REFERENCES

1) J. Ellis, Talk presented at this Workshop entitled "Exotica and expected signatures".

2) M. Shochet et al., Proceedings of the 1983 DPF Workshop on Collider Detectors: Present Capabilities and Future Possibilities, LBL-15973, p. 58.

3) ISAJET: A Monte Carlo Event Generator for pp and $\bar{p}p$ Interactions, F.E. Paige and S.D. Protopopescu.
NOTE: The calculations for jet angular width presented by F. Paige et al. in reference 2) are incorrect. The jets are too wide due to a bug subsequently found in the program.

4) J. Freeman, IEEE Trans. N.S. -29, 1, pp. 303-6 (February 1982).

5) R.N. Cahn, Proceedings of the 1983 DPF Workshop on Collider Detector: Present Capabilities and Future Possibilities, LBL-15973, p. 28.

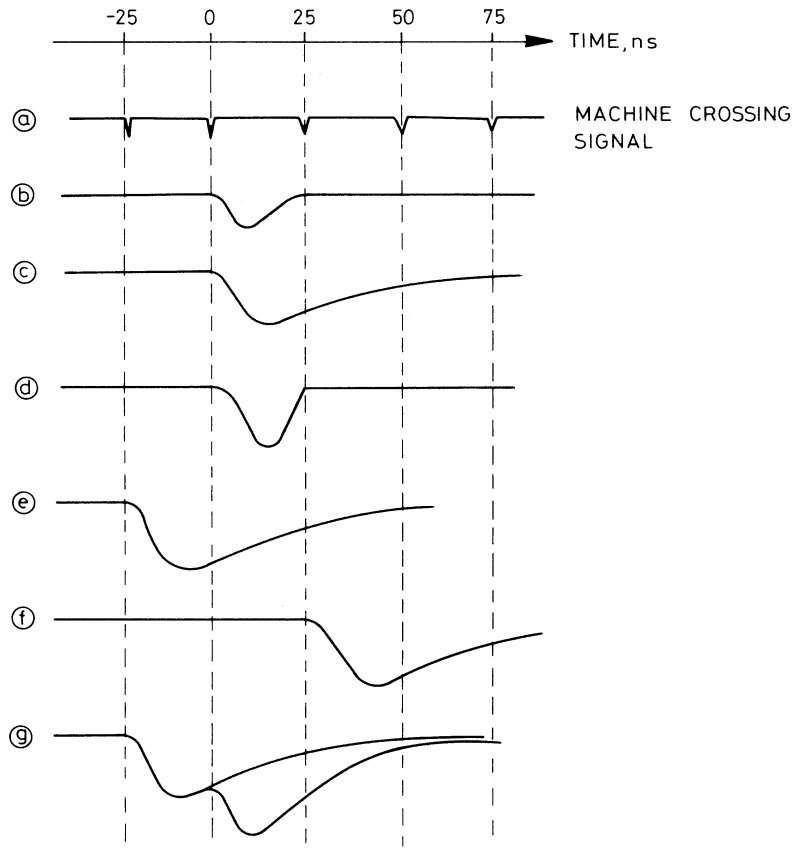

Fig. 1 Possible pulse shapes from a calorimeter cell for a bunch spacing of 25ns. Time in ns is relative to the bunch crossing under investigation.

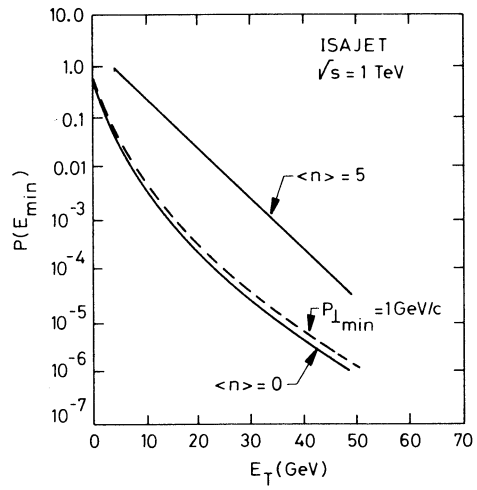

Fig. 2 Plot of transverse energy versus $P(E_{Tmin})$, the probability that <n> overlapping events give a value of $E_T > E_{Tmin}$. The solid curves are for <n> equal to 5 and 0 per crossing. The dashed curve is for <n> equal to 5 and where only calorimeter cells with $P_T > 1$ GeV/c have been included in the E_T measurement. (Figure taken from reference 2.)

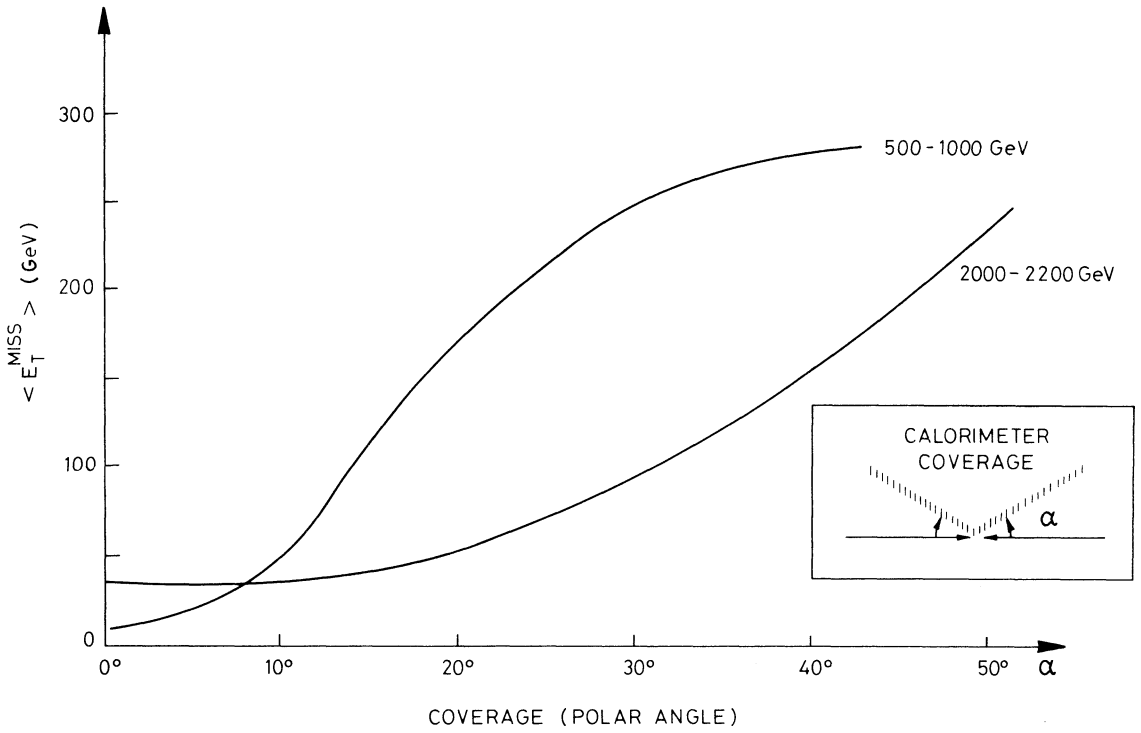

Fig. 3 Missing E_T in QCD jet events for jets in the ranges P_T = 500 - 1000 GeV/c and 2000-2200 GeV/c, as a function of calorimetry coverage (Monte-Carlo data taken from the jet working group at this workshop).

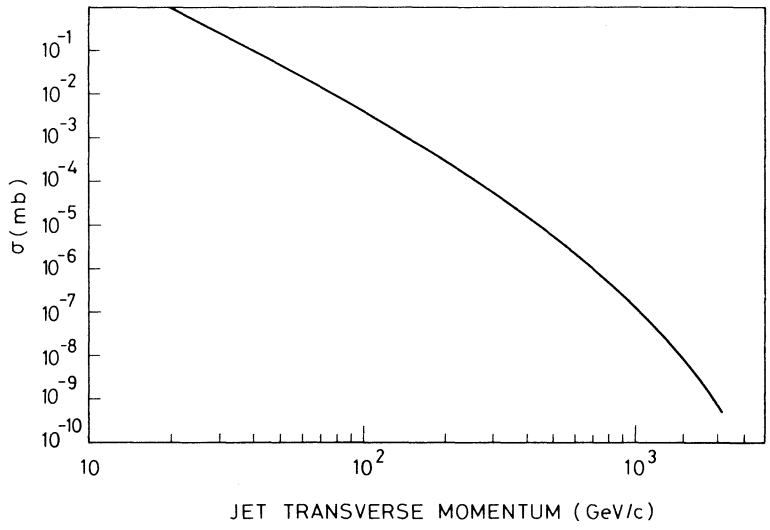

Fig. 4 Cross-section to produce a jet with transverse momentum greater than a given value, at $\sqrt{s}$ = 20 TeV. Only the subprocess gluon + gluon → gluon + gluon is considered (reference 5).

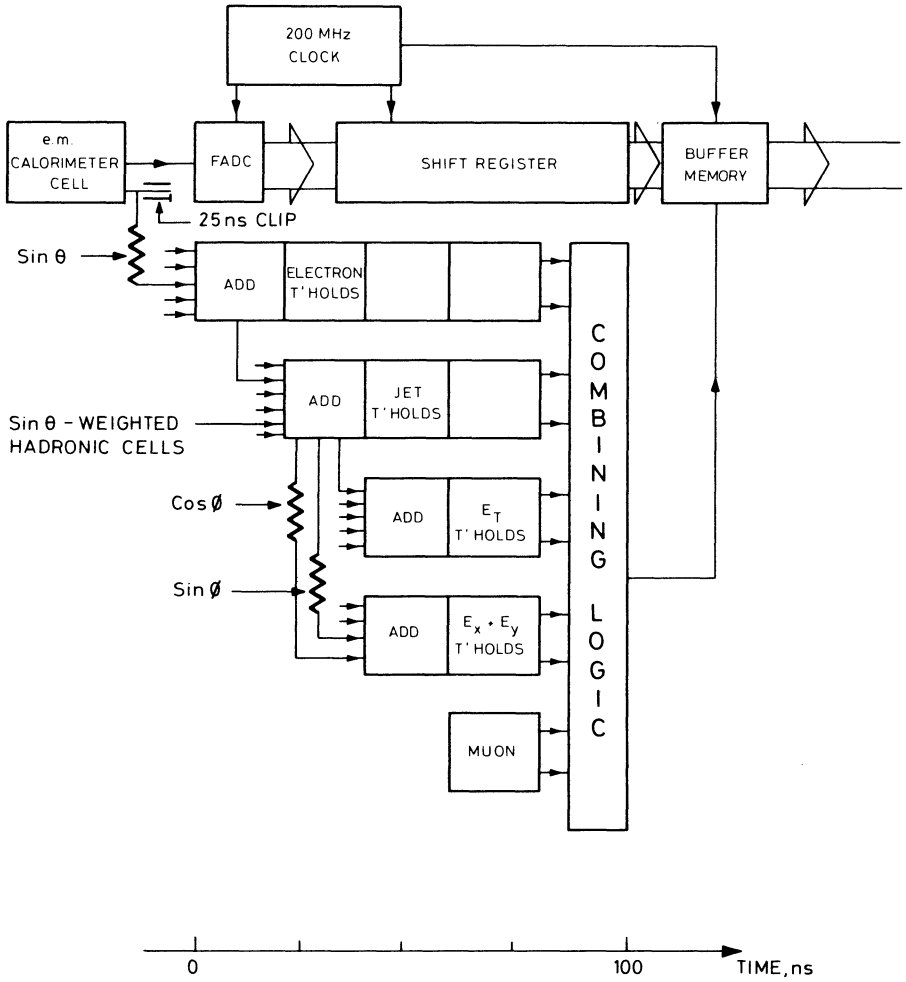

Fig. 5 Block diagram of first-level trigger processor. A decision time of $\lesssim 100$ ns can be achieved. Zero dead-time results from pipe-lining the operations on the analogue signals.

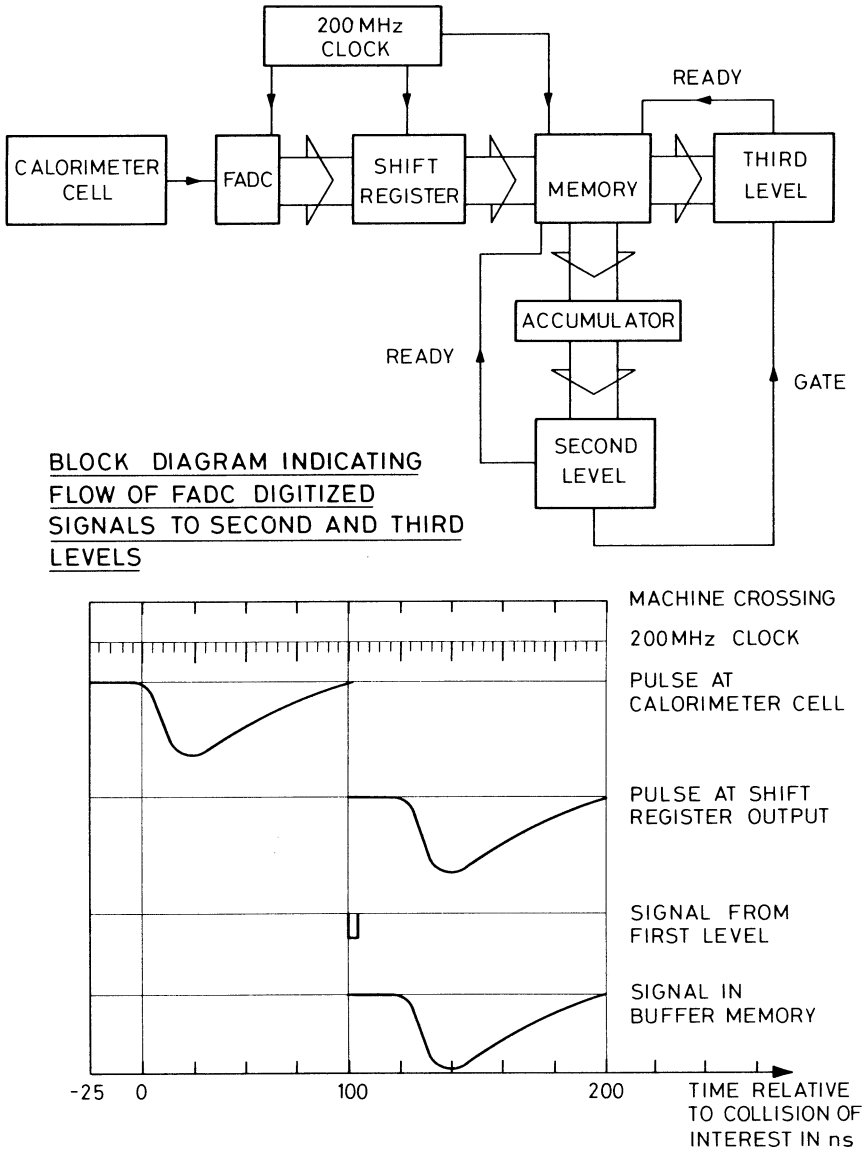

Fig. 6 Flow of digitized pulses through the second-level and third-level triggers. We have taken as an example pulses which rise and fall in 100 ns.

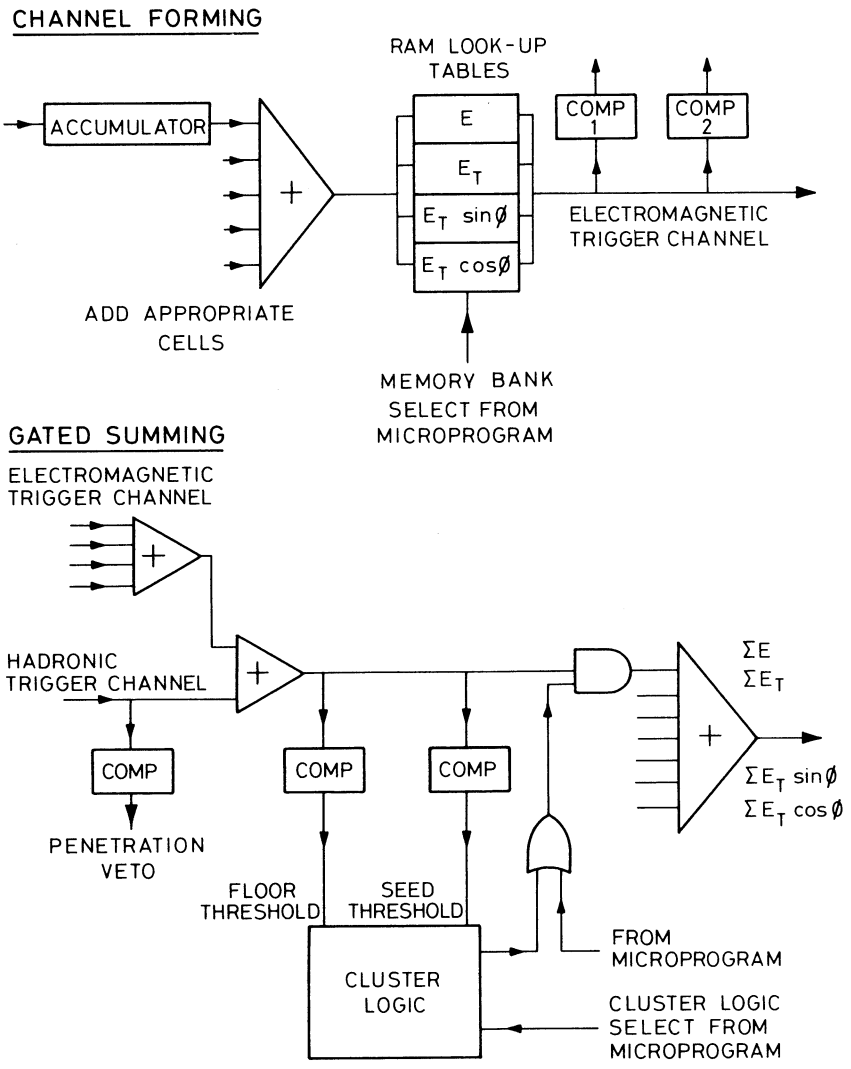

Fig. 7 Details of second-level trigger processor.